F Hautmann

Forward Backward Drell-Yan Asymmetry and PDF Determination

- Thanks to E Accomando, V Bertone, J Fiaschi, F Giuli,
  A Glazov, S Moretti, O Zenaiev and xFitter Developers' Team
  for contributed results and collaboration

- Phys Rev D98 (2018) 013003; Eur Phys J C78 (2018) 663;
  arXiv:1906.11793 [hep-ph]; work in progress

MOTIVATION

- High statistics at LHC Run II + High Luminosity runs

    --> precision physics at TeV scale (SM + BSM)

- Theoretical progress in perturbative QCD
    – finite-order calculations through NLO and NNLO
    – resummations through LL, NLL and NNLL

    --> Nonperturbative QCD contributions,
    e.g. parton distribution functions (PDFs),
    increasingly important as an essential limiting factor
    in precision studies and searches

- Which measurements will help the most to constrain PDFs and their uncertainties?

    --> "PDF profiling"

DI-LEPTON DRELL-YAN PRODUCTION MEASUREMENTS AND PDF DETERMINATION

♠ $M_{\ell\ell}$, $Y_{\ell\ell}$ $\longrightarrow$ are included in global PDF fits

♠ So is charged-current (CC) lepton charge asymmetry

♠ Triple differential cross sections $M_{\ell\ell}$, $Y_{\ell\ell}$, θ_{lepton} — not yet included
  [But see recent studies in ATLAS, JHEP 12 (2017) 059;
  C. Willis et al. (CTEQ), PRD 99 (2019) 054004]

♠ Neutral-current (NC) forward-backward asymmetry A_{FB}: traditionally used in
  precision electroweak measurements for determination of weak mixing angle θ_W
  [ATLAS, JHEP 09 (2015) 049; LHCb, JHEP 11 (2015) 190;
  CMS, PRD 84 (2011) 112002; CDF, PRD 88 (2013) 072002]

  • But present accuracy in θ_W from A_{FB} is
  an order of magnitude lower than LEP/SLD determination
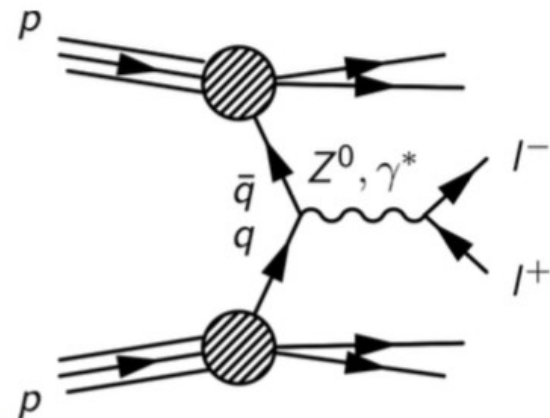 *[S. Schael et al. (Electroweak Group), Phys Rep 427 (2006) 257]*

  $\Longrightarrow$ use A_{FB} to place constraints on PDFs?
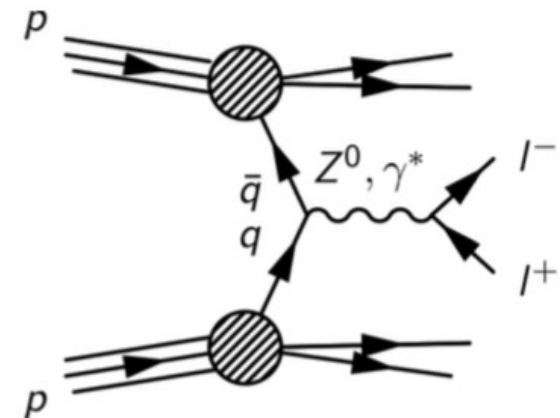
ANGULAR COEFFICIENTS IN DI-LEPTON PRODUCTION AND A_FB ASYMMETRY

Five-fold differential cross section:

$$\frac{d\sigma}{dM_{\ell\ell}dY_{\ell\ell}dP_{\ell\ell}^{\perp}d\cos\theta d\phi} = \frac{d\sigma^{(U)}}{dM_{\ell\ell}dY_{\ell\ell}dP_{\ell\ell}^{\perp}}\frac{3}{16\pi}\left[1+\cos^2\theta+\frac{1}{2}A_0(1-3\cos^2\theta)\right.$$

$$+ \ A_1\sin 2\theta\cos\phi + \frac{1}{2}A_2\sin^2\theta\cos 2\phi + A_3\sin\theta\cos\phi$$

$$+ \ A_4\cos\theta + A_5\sin^2\theta\sin 2\phi + A_6\sin 2\theta\sin\phi + A_7\sin\theta\sin\phi\left.\right]$$

Azimuthally integrated:

$$\frac{d\sigma}{dM_{\ell\ell}dY_{\ell\ell}dP_{\ell\ell}^{\perp}d\cos\theta} = \frac{d\sigma^{(U)}}{dM_{\ell\ell}dY_{\ell\ell}dP_{\ell\ell}^{\perp}}\frac{3}{8}\left[1+\cos^2\theta+\frac{1}{2}A_0(1-3\cos^2\theta)+\underbrace{A_4\cos\theta}_{\text{asymmetry}}\right]$$
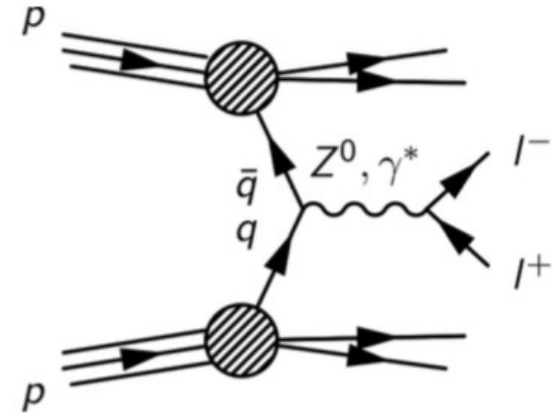
Forward-backward asymmetry:

$$A_{\text{FB}} = \frac{\sigma_F-\sigma_B}{\sigma_F+\sigma_B}$$

NB. can measure reconstructed A_FB
[*M Dittmar, PRD 55 (1997) 161*]

$$\text{where}\quad \sigma_F = \int_0^1 \frac{d\sigma}{d\cos\theta}\,d\cos\theta\ ,\quad \sigma_B = \int_{-1}^0 \frac{d\sigma}{d\cos\theta}\,d\cos\theta$$

Leading order DY differential cross section and PDF sensitivity from A_FB

LO triple differential cross section:

$$\frac{d\sigma}{dM_{\ell\ell}dY_{\ell\ell}d\cos\theta} = \frac{\pi\alpha^2}{3M_{\ell\ell}s}\sum_q H_q\left[f_q(x_1,Q^2)f_{\bar{q}}(x_2,Q^2) + \{q \leftrightarrow \bar{q}\}\right]$$

where H_q is given in terms of the vector and axial couplings v and a and electric charges e by

$$
\begin{aligned}
H_q =\ & e_\ell^2 e_q^2(1+\cos^2\theta) && \gamma \text{ exchange}\\
+\ & e_\ell e_q \frac{2M_{\ell\ell}^2(M_{\ell\ell}^2 - M_Z^2)}{\sin^2\theta_W\cos^2\theta_W\left[(M_{\ell\ell}^2 - M_Z^2)^2 + \Gamma_Z^2 M_Z^2\right]}\left[v_\ell v_q(1+\cos^2\theta) + 2a_\ell a_q\cos\theta\right] && \\
& && Z/\gamma \text{ interference}\\
+\ & \frac{M_{\ell\ell}^4}{\sin^4\theta_W\cos^4\theta_W\left[(M_{\ell\ell}^2 - M_Z^2)^2 + \Gamma_Z^2 M_Z^2\right]}\left[(a_\ell^2 + v_\ell^2)(a_q^2 + v_q^2)(1+\cos^2\theta) + 8a_\ell v_\ell a_q v_q\cos\theta\right] && \\
& && Z \text{ exchange}
\end{aligned}
$$

- A_{FB} dominated by Z/γ interference $\cos\theta$ term proportional to $e_\ell e_q a_\ell a_q$, with $a_q = T_3/2$

$$A_{\mathrm{FB}} \text{ predominantly sensitive to } \frac{2}{3}u + \frac{1}{3}d$$
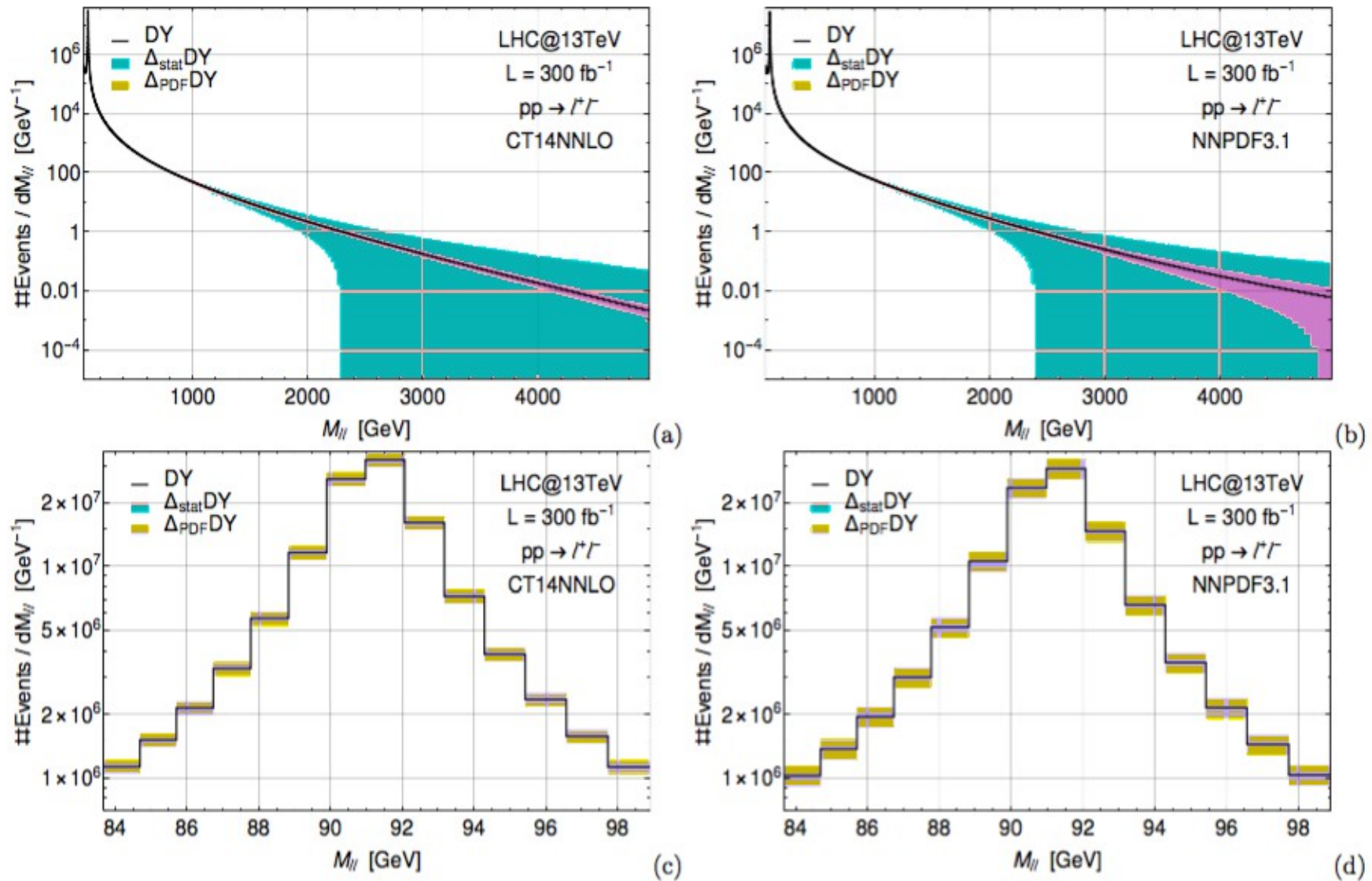
The Cross Section Case

FIG. 1: (a) Expected number of events in the di-lepton invariant mass region and their statistical and PDF error obtained with CT14NNLO. (b) Same as (a) obtained with NNPDF3.1. (c) Zoom of (a) around the Z-boson peak. (d) Zoom of (b) around the Z-boson peak.

- high-M region dominated by statistical uncertainties – exploit high statistics for M near M_Z
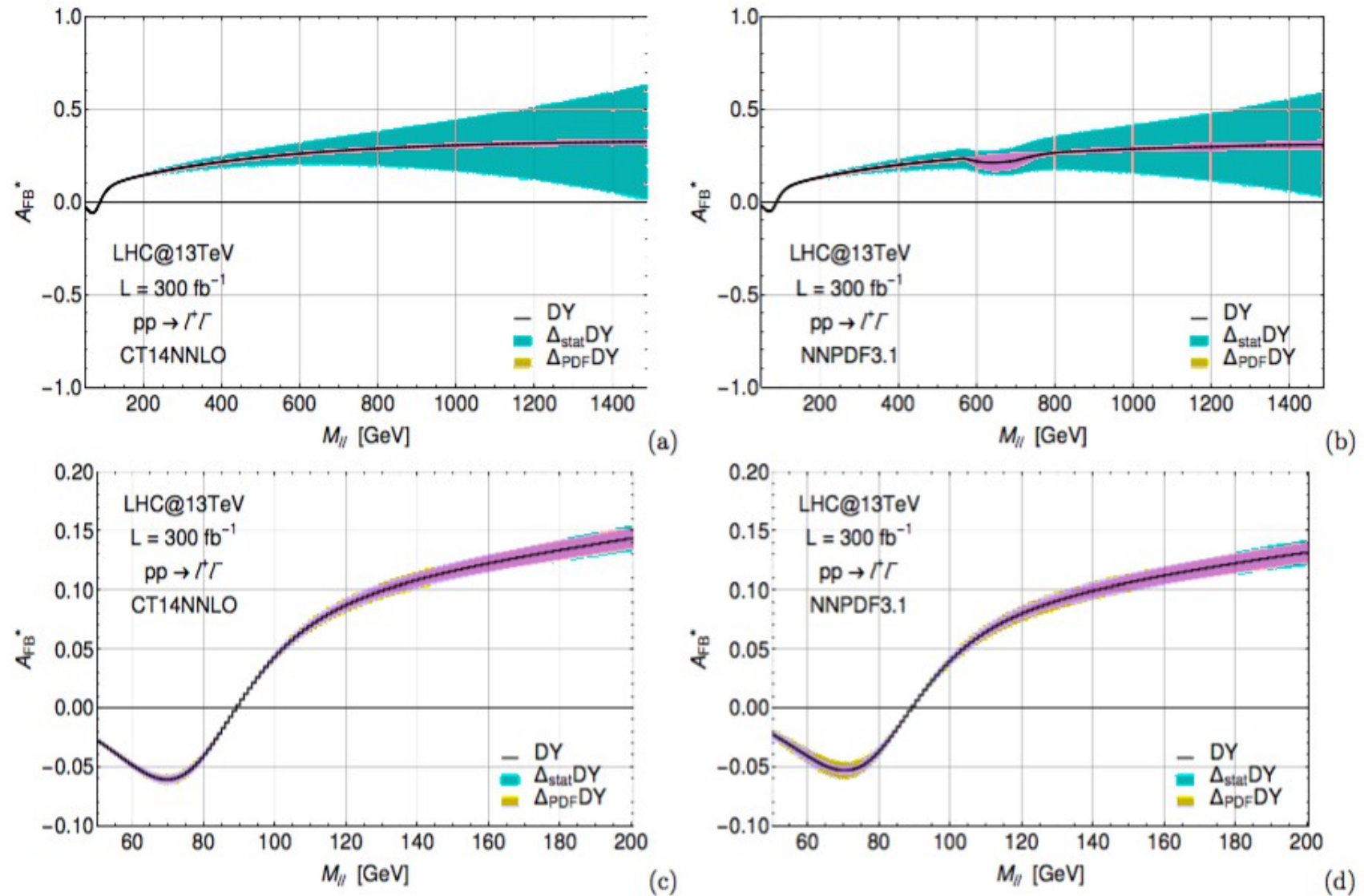
The A_FB Asymmetry Case

FIG. 2: (a) A^*_{FB} distribution in the di-lepton invariant mass including the statistical and PDF errors obtained with CT14NNLO. (b) Same as (a) for the NNPDF3.1 PDF set. (c) Zoom of (a) around the Z-boson peak. (d) Zoom of (b) around the Z-boson peak.

- here too the high-M region is affected by large statistical uncertainties – exploit low-M region
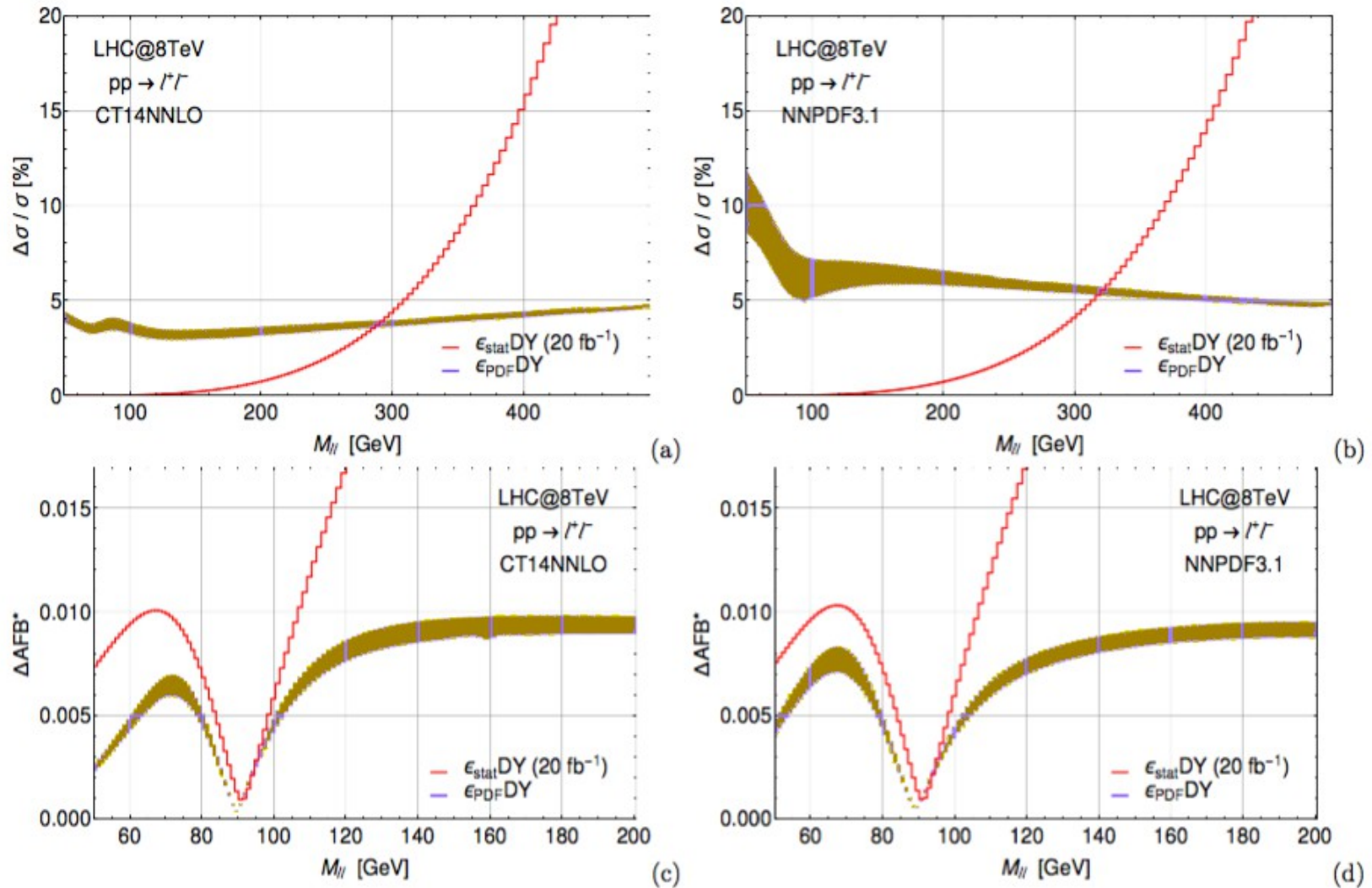
Run I Legacy

FIG. 3: (a) Relative errors on the differential cross section at the LHC Run-I with $\sqrt{s} = 8$ TeV and $L = 20$ fb^{-1}, computed with the CT14NNLO PDF set. The red curve represents the statistical error. The blue band has been obtained evaluating the PDF error fixing the factorization/renormalization scale in the interval: $0.5 M_{\ell\ell} < Q < 2 M_{\ell\ell}$. (b) Same as (a) for the NNPDF3.1 PDF set. (c) Absolute errors on the reconstructed FB asymmetry at the LHC Run-I, computed with the CT14NNLO PDF set. The red curve represents the statistical error. The blue band refers to the PDF uncertainty. (d) Same as (c) for the NNPDF3.1 PDF set.

- the two sources of uncertainty are comparable → no gain in PDF determinations from including A_FB at Run I
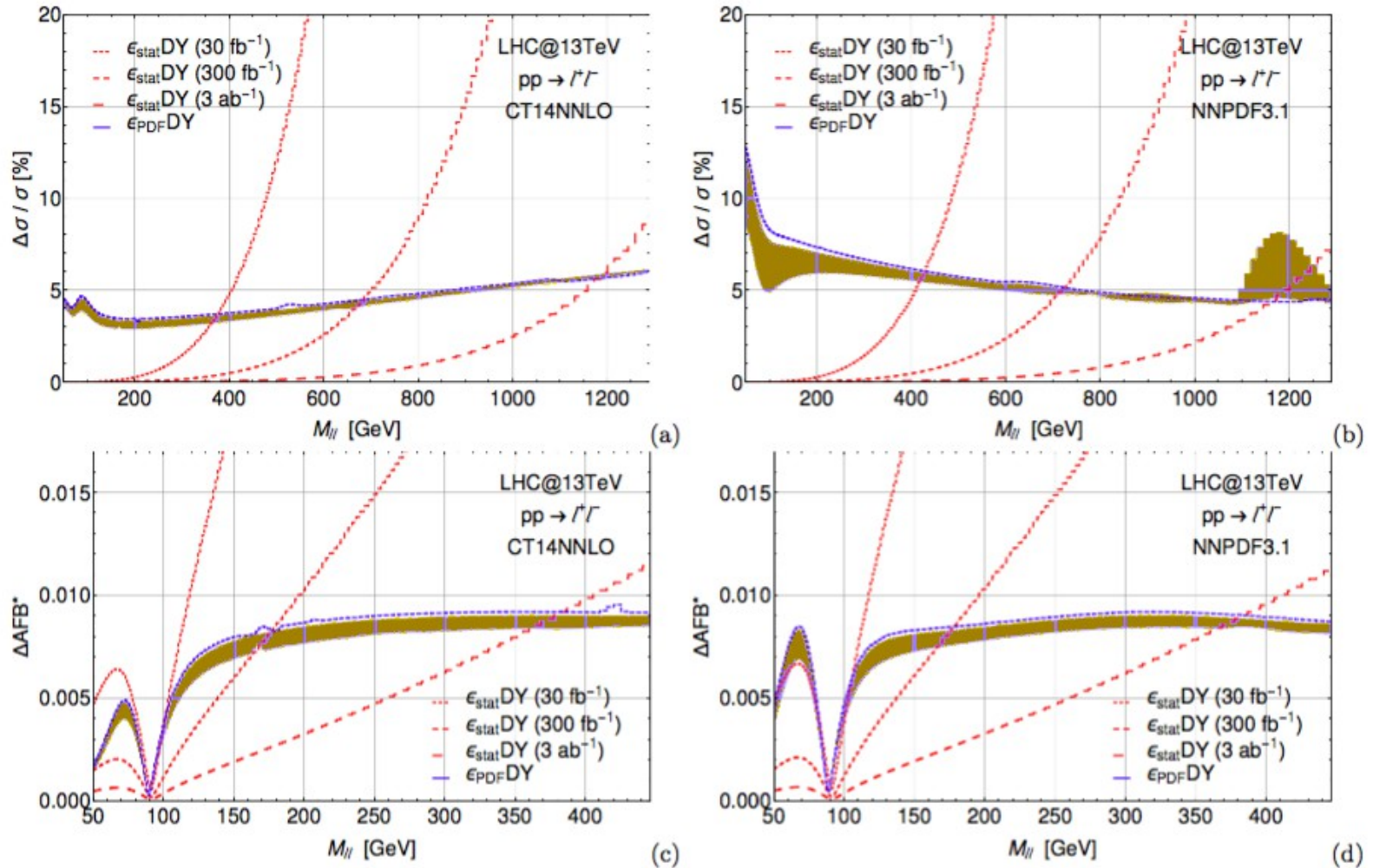
Run II and HL LHC

FIG. 4: (a) Relative size of statistical error and PDF uncertainty on the differential cross section obtained with the CT14NNLO set at the 13 TeV LHC. The statistical error is displayed for three different values of the luminosity (see legend). The PDF error band has been obtained evaluating the PDF error fixing the factorization/renormalization scale in the interval: $0.5 M_{\ell\ell} < Q < 2 M_{\ell\ell}$, while the dashed blue lines represent the PDF uncertainty obtained fixing $\mu_F = \mu_R = p_T$, with p_T the transverse momentum of either lepton in the final state. (b) Same as plot (a) for the NNPDF3.1 PDF set. (c) Absolute value of statistical and PDF uncertainties on the reconstructed A_{FB}^* distribution obtained with CT14NNLO. The statistical error is obtained with the integrated luminosities of 30 fb^{-1}, 300 fb^{-1} and 3 ab^{-1}. The PDF error bands and lines follow the conventions of plots (a) and (b). (d) Same as (c) for the NNPDF3.1 PDF set.

• regions in which sigma and A_FB data can improve PDF determinations arise at Run II and HL LHC

F Hautmann: LHC EW Meeting - CERN, 1 July 2019   9

PDF profiling - using A_FB

Setup of xFitter analysis

Datafiles with <u>pseudo-data</u> generated for many PDF sets with the following setup:

- AFB central values:
  120 bins of 1 GeV from 80 GeV to 200 GeV.
- Estimation of statistical uncertainty:
  at different integrated luminosities (*30 fb⁻¹, 300 fb⁻¹* and *3000 fb⁻¹*)
  including detector acceptance and efficiency in the di-electron final state.
- Rapidity cuts:
  different lower rapidity cuts applied (*|Y| > 0, |Y| > 0.8* and *|Y| > 1.5*)

Profiling exercise performed on 5 NNLO PDF sets:
ABMP16NNLO, CT14NNLO, HERA2.0NNLO, MMHT2014NNLO, NNPDF3.1NNLO (hessian set).

Results will be shown for 2 reference scales $Q^2 = 100$ GeV^2 and $Q^2 = M_z^2$ GeV^2.

Reweighted eigenvectors are returned by xFitter and analysed with the **xFitter-draw** script.

[*S Alekhin et al, Eur Phys C75 (2015) 304*]

NLO QCD corrections computed from MadGraph5_aMC@NLO, interfaced to APPLgrid via aMCfast
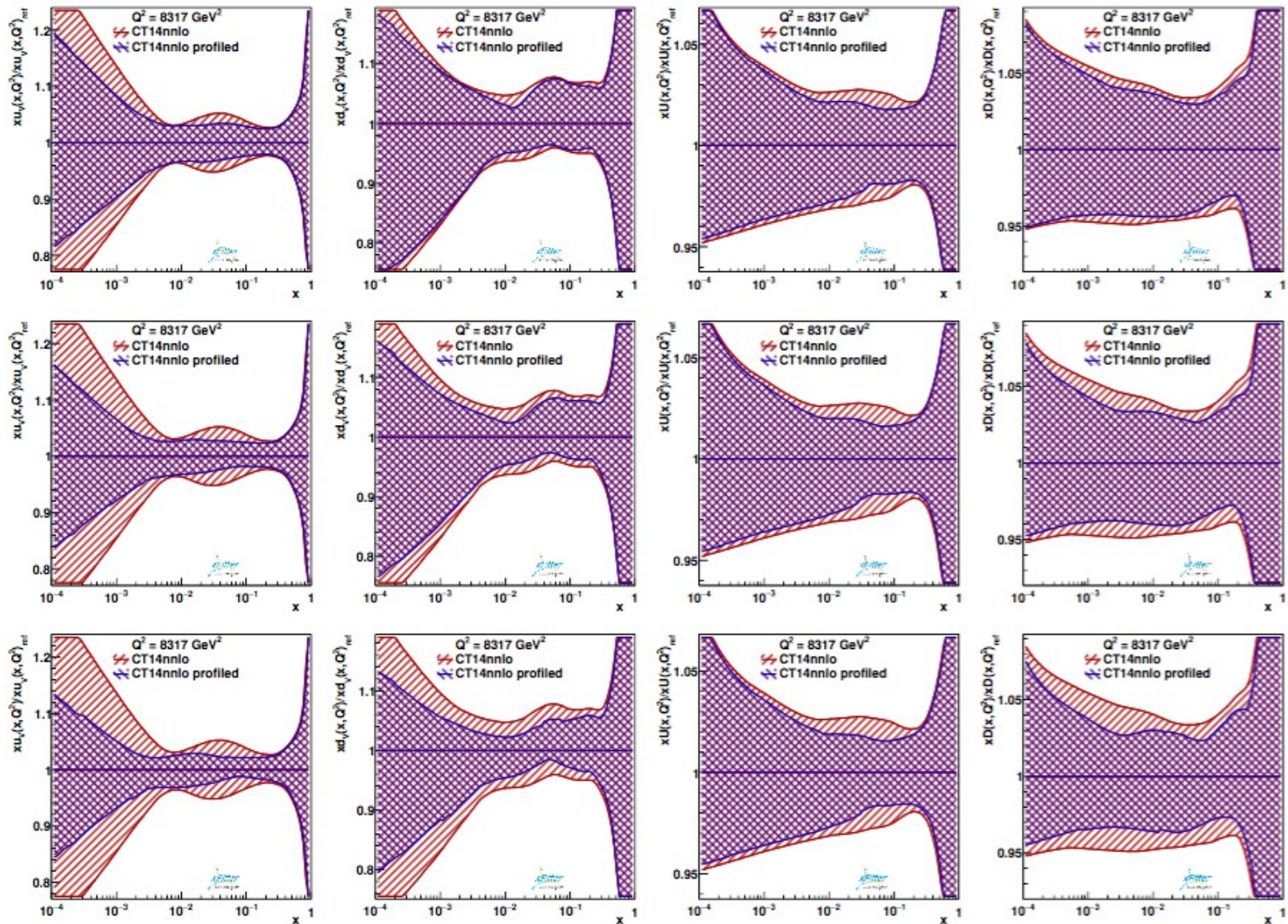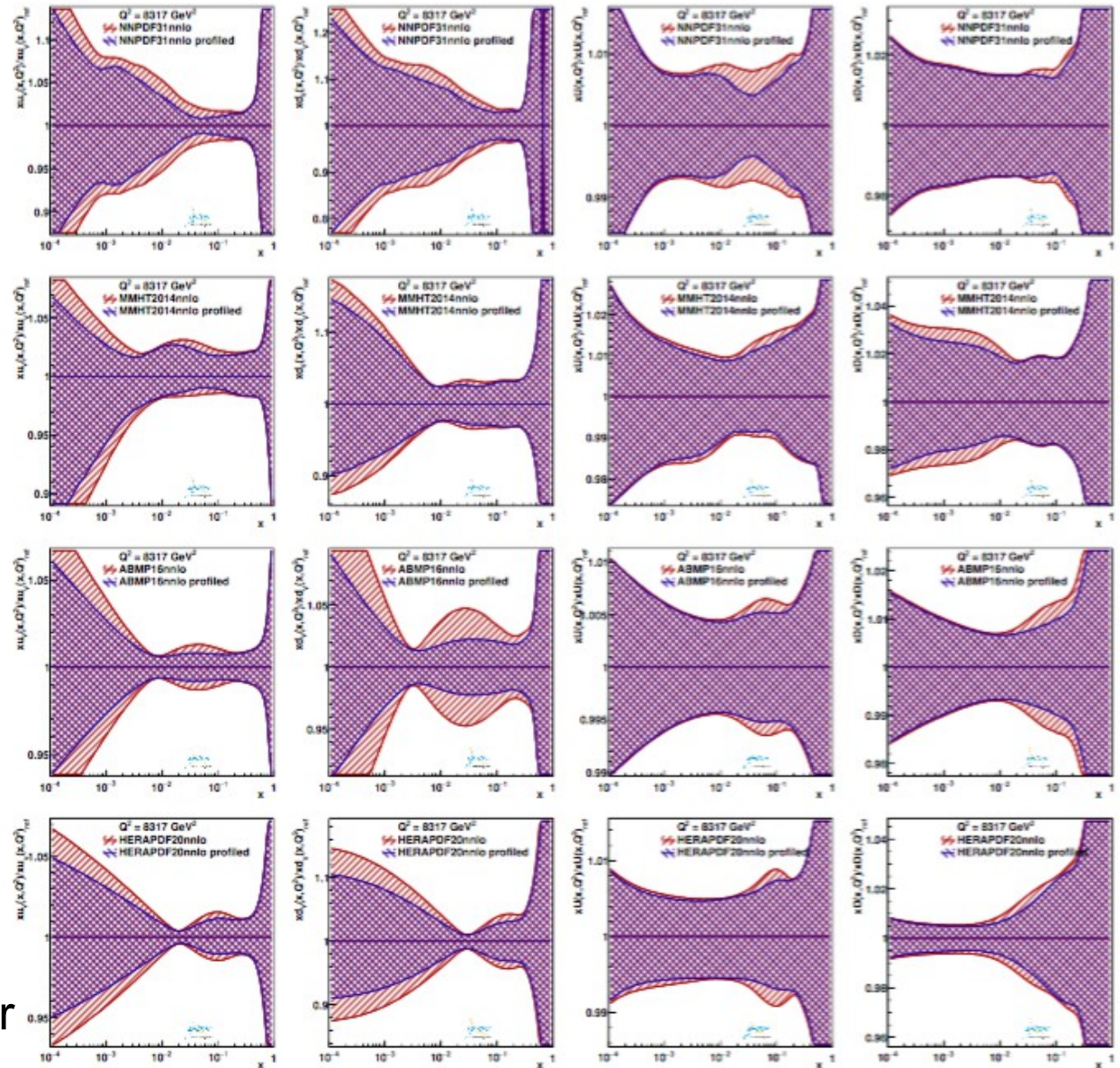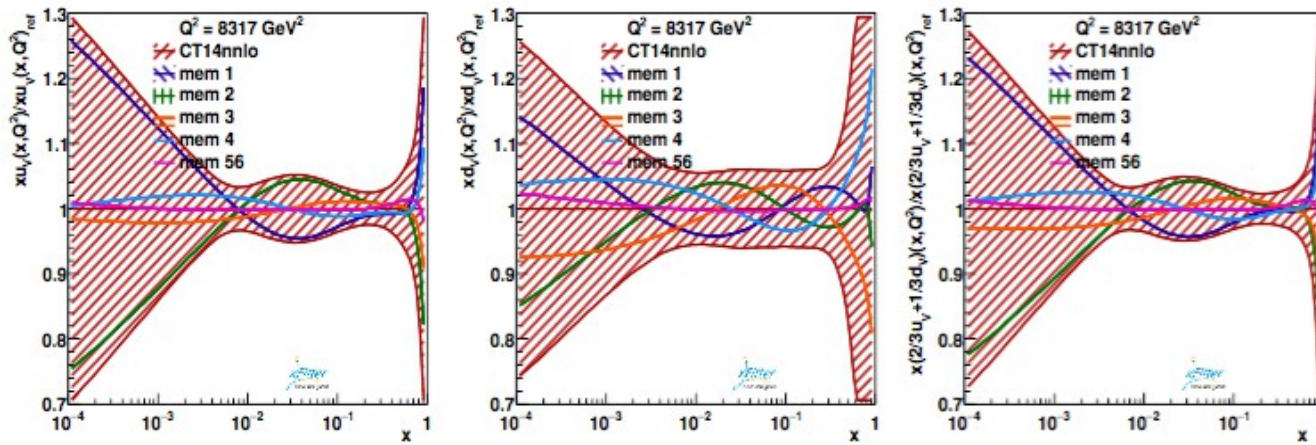
PDF profiling - using A_FB

FIG. 1: Original (red) and profiled (blue) distributions for the normalised distribution of the ratios of (left to right) u-valence, d-valence, u-sea and d-sea quarks of the CT14nnlo PDF set. The profiled curves are obtained using A_{FB}^* pseudodata corresponding to an integrated luminosity of (rows top to bottom) 30 fb^{-1}, 300 fb^{-1} and 3000 fb^{-1}.

- largest reduction of uncertainty band for u-valence at intermediate to low x; also for d-valence and sea as luminosity grows

PDF profiling - using A_FB

- Impact of A_FB differs for different PDF sets

- ABMP16, CT14 and HERA2.0 are the most sensitive to A_FB

- Can probe higher x by employing cuts in rapidity

- Investigate which PDFs are most sensitive via eigenvector re-parameterisation (for sets with Hessian eigenvectors, CT14 and HERA2.0) ↪

FIG. 2: Original (red) and profiled (blue) distributions for the normalised distribution of the ratios of (left to right) u-valence, d-valence, u-sea and d-sea quarks. The profiled curves are obtained using A_{FB}^* pseudodata corresponding to an integrated luminosity of 300 fb^{-1}. Distributions are shown for the PDF sets (rows top to bottom) NNPDF3.1nnlo, MMHT2014nnlo, ABMP16nnlo and HERA2.0nnlo.

Eigenvector rotation

Figure 6. Contribution of the first four and last rotated eigenvectors to the uncertainty error bands of the normalised distribution of the ratios of (left to right) u-valence, d-valence and $((2/3)u + (1/3)d)$-valence of the CT14nnlo PDF set. The eigenvectors are rotated and sorted according to their sensitivity to A^*_{FB} pseudodata corresponding to an integrated luminosity of 300 fb^{-1}.

• First two eigenvectors almost completely determine the error band
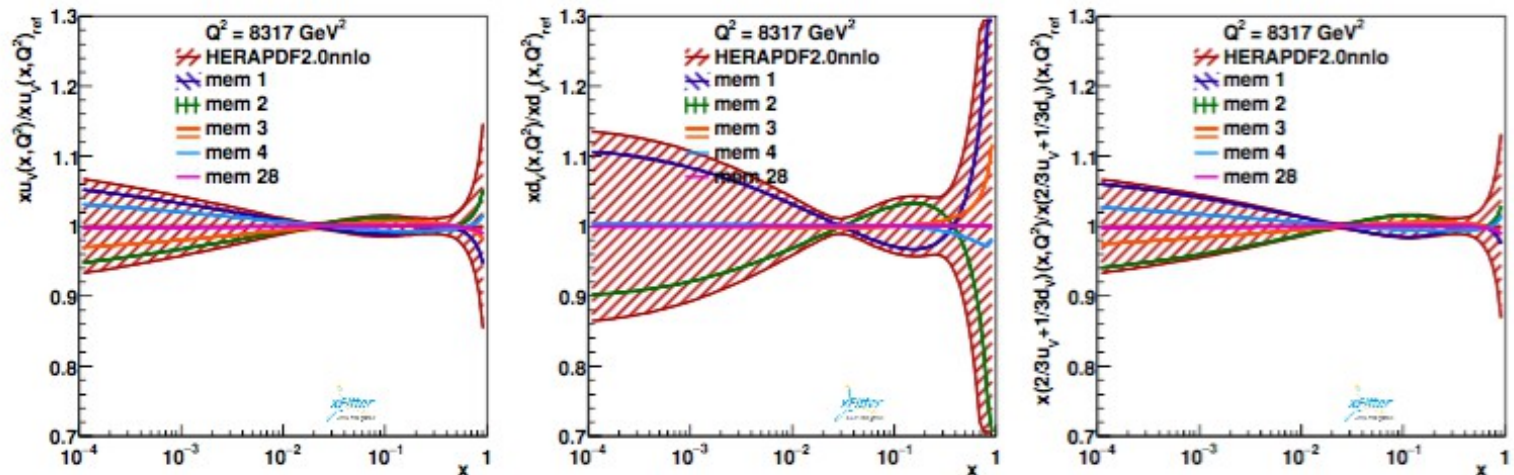
• Strongest constraints on charge-weighted sum of u-valence and d-valence

Parton luminosities at high rapidity

- High rapidity cut suppresses d dbar interactions and gives us a handle on u and ubar

- Selecting Y = 4.5 on the Z pole we have an overall contribution from d dbar processes of
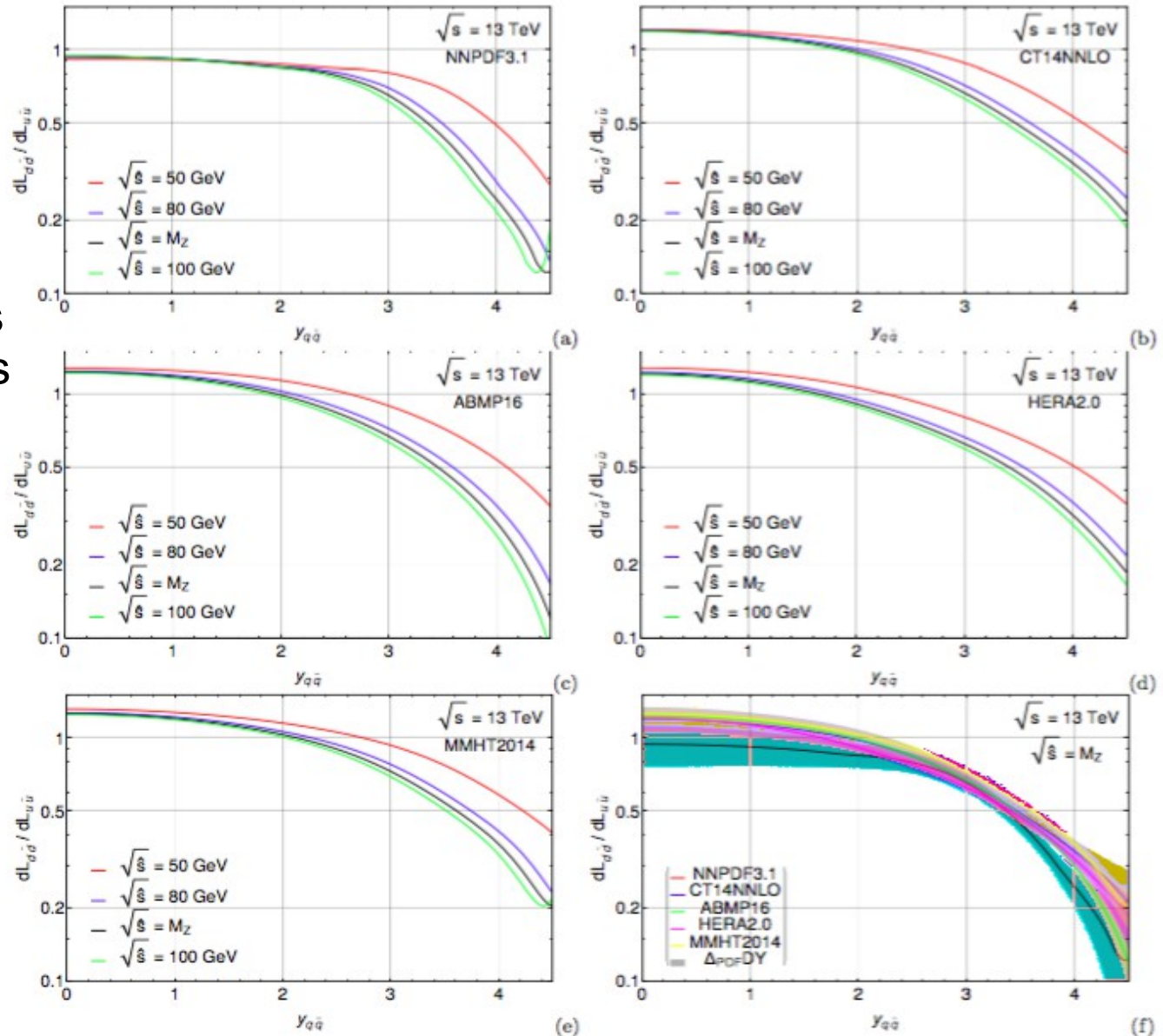

FIG. 4: Ratio of the $d - \bar{d}$ and $u - \bar{u}$ parton luminosities as a function of the c.o.m. rapidity at four fixed values of the c.o.m. energy and for the PDF sets (a) NNPDF3.1, (b) CT14, (c) ABMP16, (d) HERA2.0, (e) MMHT2014. (f) Same ratio including the PDF error band for all the sets at fixed energy $\sqrt{\hat{s}} = M_Z$.

NNPDF: 2% - 23%   **CT14:** 13% - 29%   **ABMP:** 10% - 14%   **HERA:** 14% - 23%   **MMHT:** 16% - 25%

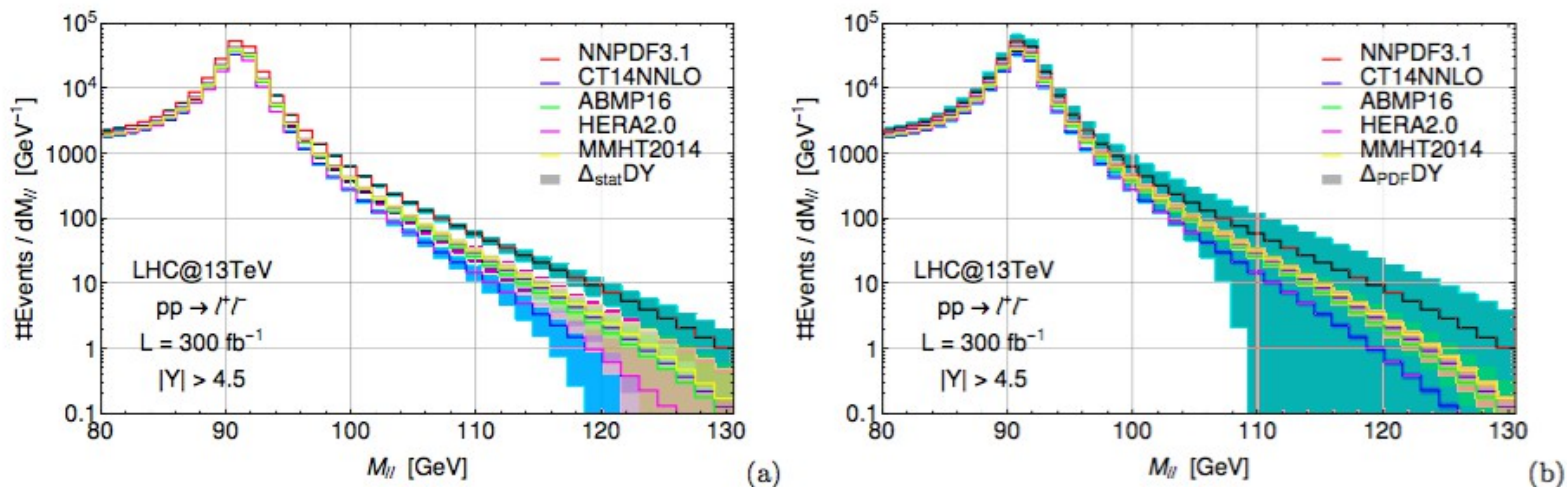# u and ubar sensitivity: the high rapidity case

FIG. 5: Number of events as a function of the di-lepton invariant mass including the (a) statistical and (b) PDF errors for a rapidity cut $|Y_{ll}| > 4.5$. A luminosity $L = 300$ fb^{-1} is assumed and acceptance cuts $|\eta| < 5$ and $p_T > 20$ GeV are imposed on both leptons.
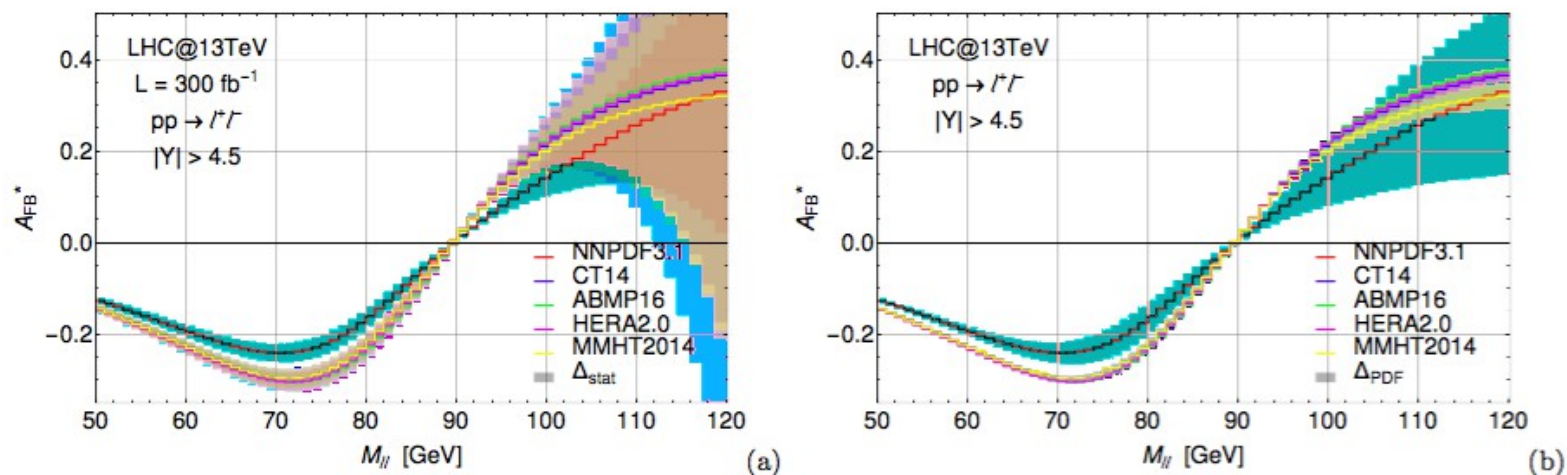

FIG. 6: A_{FB}^* as a function of the di-lepton invariant mass including the (a) statistical and (b) PDF errors with a rapidity cut $|y| > 4.5$. A luminosity $L = 300$ fb^{-1} is assumed and acceptance cuts $|\eta| < 5$ and $p_T > 20$ GeV are imposed on both leptons.

- In high rapidity region A_FB is helpful to disentangle different PDF sets
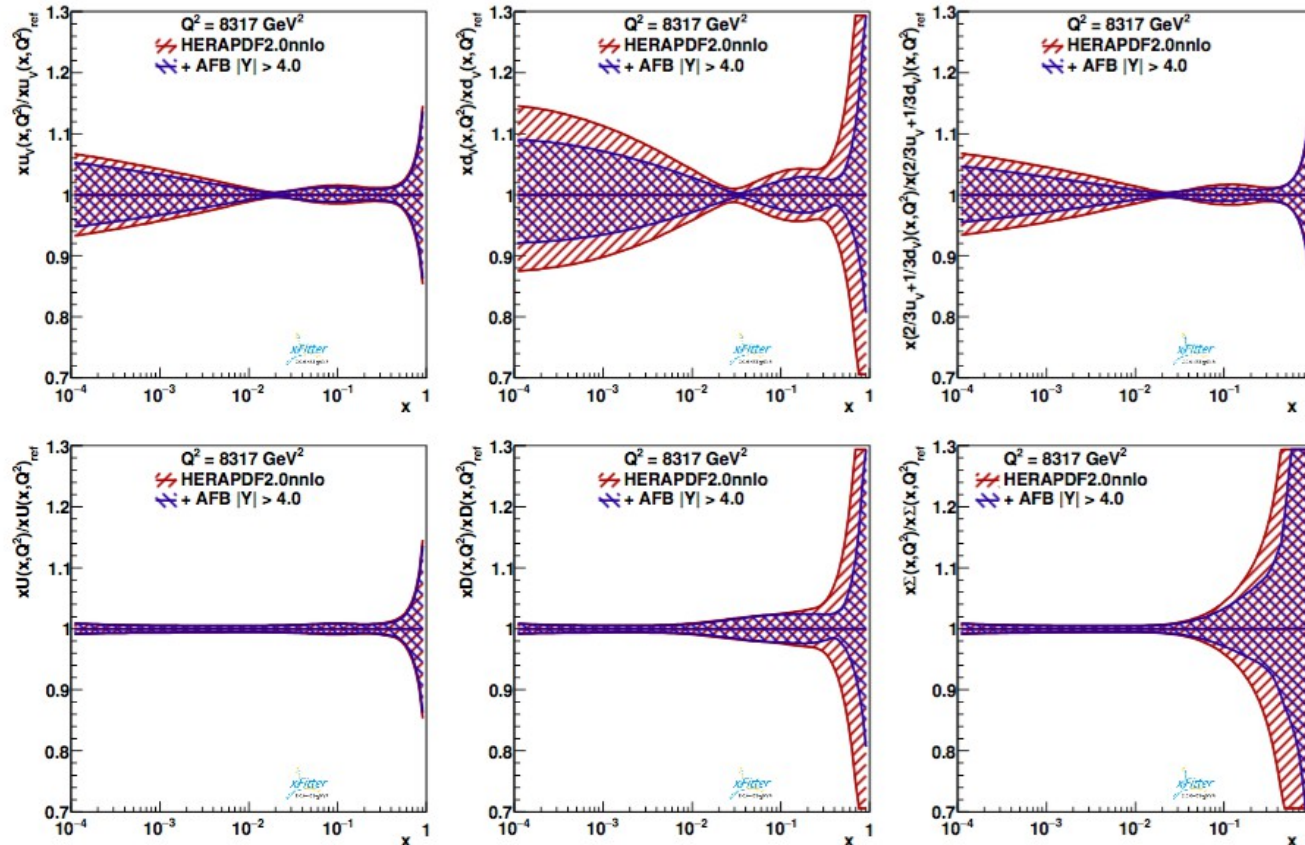
Profiling with high rapidity cut

Figure 5. Original (red) and profiled (blue) distributions for the normalised distribution of the ratios of (top row, left to right) u-valence, d-valence and $((2/3)u + (1/3)d)$-valence and (bottom row, left to right) u-sea, d-sea quarks and $(u + d)$-sea quarks of the HERAPDF2.0nnlo PDF set obtained using A^*_{FB} pseudodata corresponding to an integrated luminosity of 3000 fb^{-1}, applying a rapidity cut of $|y_{\ell\ell}| > 4.0$. The acceptance region of the detector has been enlarged up to $|\eta_\ell| < 5$, and the profiling is performed through the LO code.

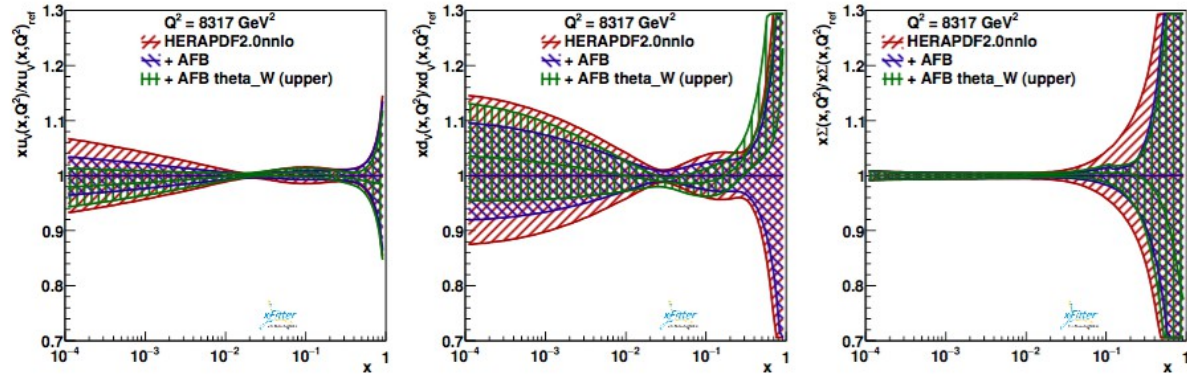# Systematic theta-W effects: LEP/SLD vs. global EW fit

Figure 9. Profiled curves obtained using the upper limit of $\sin^2 \theta_W$ allowed by LEP-SLD measurements. The pseudodata corresponds to an integrated luminosity of 3000 fb^{-1}.
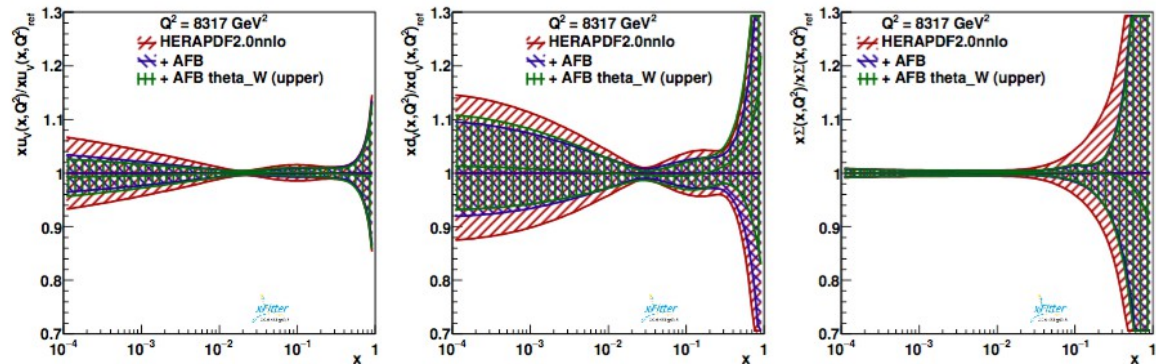

Figure 10. Profiled curves obtained using the upper limit of $\sin^2 \theta_W$ allowed by the estimation from a global fit of electroweak parameters. The pseudodata corresponds to an integrated luminosity of 3000 fb^{-1}.

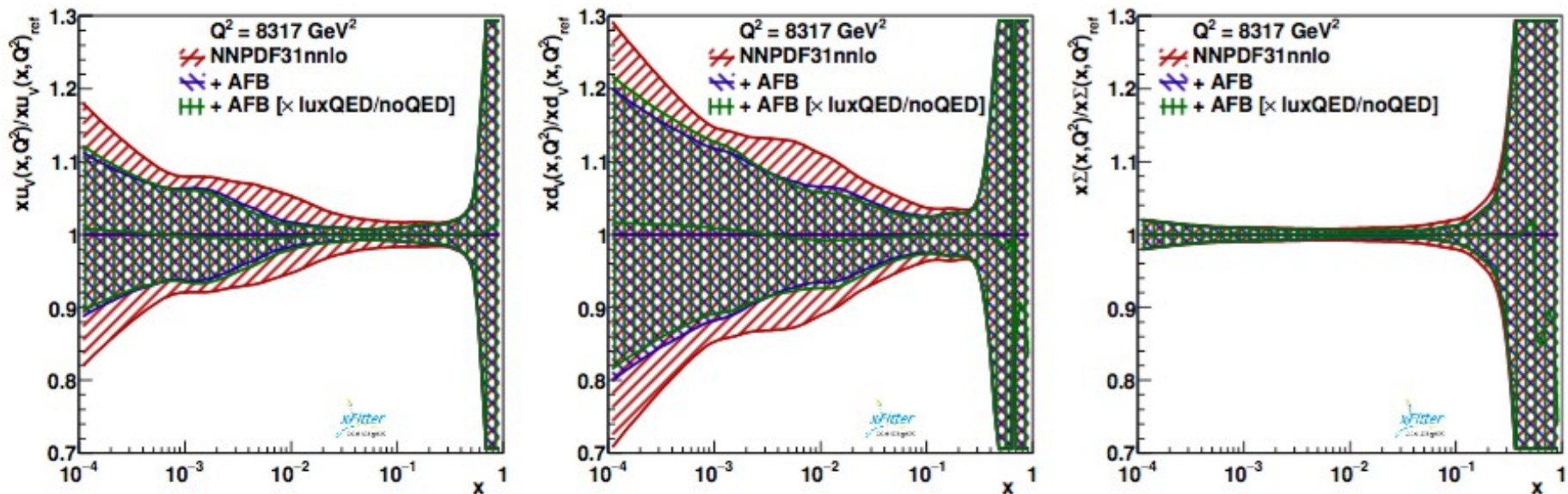# Studying impact of QED PDFs on profiling via k-factor

Figure 11. Profiled curves obtained with the NNPDF3.1nnlo and its central value predictions rescaled with a K-factor to match the NNPDF31_nnlo_as_0118_luxqed predictions. The pseudo-data corresponds to an integrated luminosity of 3000 fb^{-1}.

Missing electroweak corrections: impact of Z peak and W W threshold regions
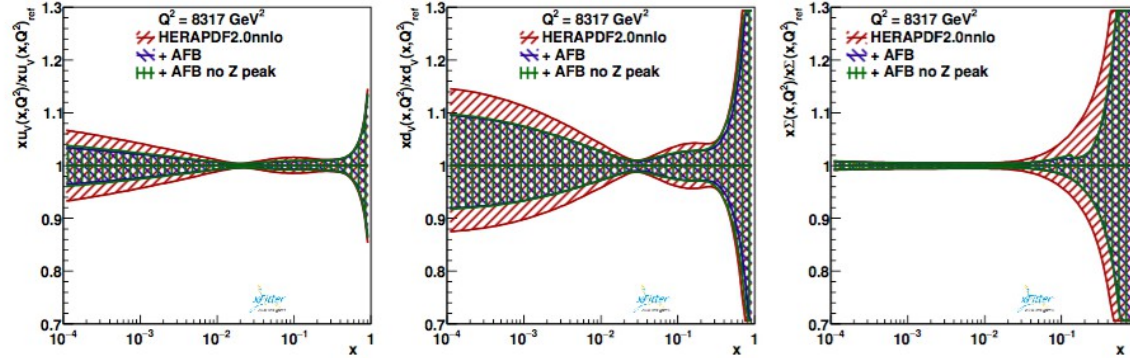

Figure 12. Profiled curves obtained with the HERAPDF2.0nnlo using the full set of data, and when removing the data in the invariant mass region around the Z peak. The pseudodata corresponds to an integrated luminosity of 3000 fb^{-1}.
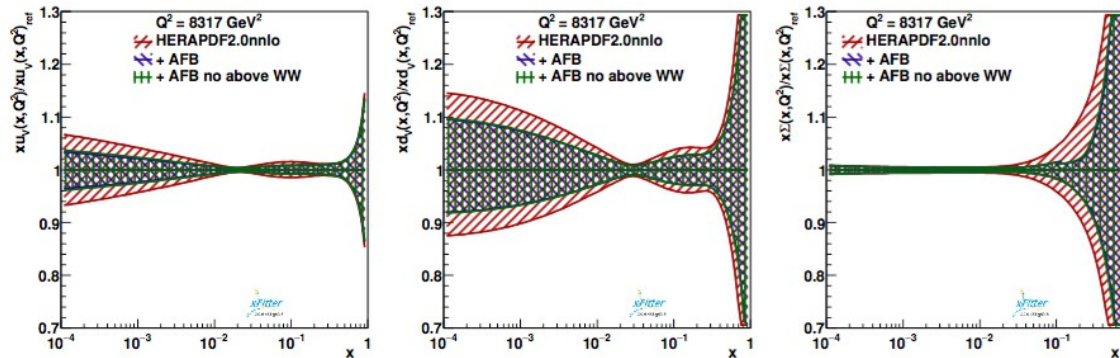

Figure 13. Profiled curves obtained with the HERAPDF2.0nnlo using the full set of data, and when removing the data in the invariant mass region above WW production threshold. The pseudodata corresponds to an integrated luminosity of 3000 fb^{-1}.

Concluding remarks

Using high luminosity measurements to constrain
nonperturbative QCD effects from PDFs
is one of upcoming LHC goals

- PDF profiling tools instrumental to this – xFitter is one such tool

- New PDF sensitivity by associating to di-lepton M_ll and
  Y_ll spectra the NC forward-backward asymmetry, encoding
  lepton's angular information

- Will be primary avenue in coming years for reducing PDF (and
  "PDF set") uncertainty